

模拟真实水体环境下目标激光点云数据的三维重建与分析

王明军^{1*}, 李乐¹, 易芳¹, 雷小博²

¹西安理工大学自动化与信息工程学院, 陕西 西安 710048;

²西安理工大学工程训练中心, 陕西 西安 710048

摘要 水下目标探测在水下事故搜救、设备维护以及资源勘探等领域有重要的应用。通过实验模拟了两种典型海域的水体环境,研究了盐度和浊度这两个水体物理特性参数以及探测距离对水下潜艇、滑翔机和锚雷的激光点云三维重建效果的影响,并将重建后的三维点云数据和三种模型的标准点云进行对比并分析误差。结果表明:盐度变化对水下目标三维点云重建的影响较小,平均误差变化范围在 1 mm 以内;浊度增大会增强水体的后向散射影响,对成像有较大的干扰,有效点数显著减少;随着探测距离的增大,均值误差呈线性上升,目标点云图像的轮廓变得模糊。

关键词 图像处理; 水下探测; 真实水体模拟; 三维点云重建; 误差分析

中图分类号 TN29 **文献标志码** A

doi: 10.3788/CJL202249.0309001

1 引言

海洋面积约占地球总面积的 71%,目前主要利用水声探测技术进行水下探测,存在分辨率低、目标边缘模糊、形状畸变等问题,往往难以有效识别目标,无法满足油气管道(dm 量级),水下电缆(cm 量级),水下渔网避障(mm 量级),失事轮船、飞机和 underwater 文物等识别的应用需求^[1-3]。水下光学探测系统的高光学频率能提高探测目标的分辨率,并实现实时成像,能够弥补声呐探测技术的不足^[4-6]。真实海洋水体环境往往受盐度、温度和浊度等物理特性的影响^[7-8],水下光学探测系统的工作环境较为恶劣^[9-10],从而影响系统的探测精度。因此,研究真实水体物理特性改变对探测结果的影响极为重要,其对相关设备的设计研发具有重要意义。

在海洋中进行水下探测实验较为困难,因此在实验室里通过控制不同水体环境变化来模拟真实水体环境的研究极有意义。早在 1993 年,Fournier

等^[11]分别在水箱和加拿大港口附近的水域中测试了 LUCIE 系统的性能,该系统的探测范围是传统泛光相机的 3~5 倍。Busck 等^[12]设计了一种门控激光雷达成像系统,分别在实验室环境下的清水和淡海水中获取了 3D 图像,其中淡海水的盐度在 15‰左右,成像范围在 4~5 m。Dalgleish 等^[13]基于激光线扫描技术设计了一款水下成像系统,其通过在水罐中添加氢氧化镁来控制水体浊度,分析了其系统的性能。查冰婷^[14]分别在清水水体和 35 PSU(即每千克海水的含盐量为 35 克,也用 35‰表示)水体中测试了其设计的水下周向扫描系统,总体上 35 PSU 水体比清水水体的有效探测距离减小了 3 m。Xie 等^[15]研制了一种深海激光线扫描系统,在实验室水罐和深海中进行成像实验,结果显示,在 2 m×2 m×1 m 的范围内,两种水体的成像误差均小于 3 mm。Qian 等^[16]通过向水池中添加牛奶来模拟实际水下环境中悬浮颗粒的吸收与散射,通过实验证明了近红外光比可见光具有更强的

收稿日期: 2021-05-08; 修回日期: 2021-06-08; 录用日期: 2021-06-18

基金项目: 国家自然科学基金重大研究计划培育项目(92052106)、国家自然科学基金(61771385)、陕西省杰出青年科学基金(2020JC-42)

通信作者: *wmjxd@aliyun.com

通过浑浊介质传输成像信息的能力。

本文依据典型海域的实际参数,模拟了两种真实水体的物理特性,分析了盐度和浊度变化对水下潜艇、滑翔机和锚雷模型的三维点云重建图像的影响采用阈值分割、折射修正和噪声滤除算法对实验所得到的原始点云数据进行处理,得到只包含目标物的三维点云图像,并与 3Dmax 软件建模处理后的标准点云作误差运算,数据化展示了盐度、浊度以及探测距离对点云重建图像的有效点数和均值误差的影响。

2 真实水体环境模拟及点云数据三维重建

2.1 水下目标探测实验设计

实验在长、宽、高分别为 100 cm、50 cm、50 cm 的玻璃水槽中进行,向水槽中注入清水,激光雷达紧贴水槽放置在水槽一端,其探测波长为 850 nm,最大帧

度为 54 frame/s,成像分辨率为 176 pixel \times 144 pixel,标准视角为 43.6 $^{\circ}$ \times 34.6 $^{\circ}$,被探测目标由重物悬挂至水体中央固定,利用激光雷达收集原始点云数据。图 1 为所设计的水下目标探测实验装置示意图。

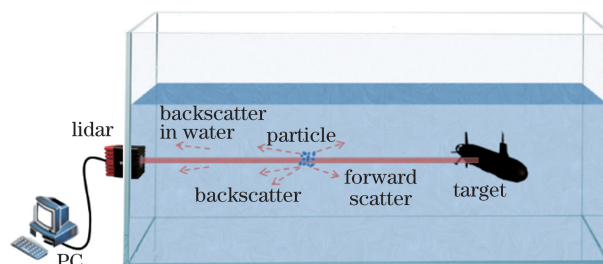


图 1 水下目标探测实验装置示意图

Fig. 1 Schematic of underwater target detection experiment device

被探测目标为自行设计打印的潜艇、水下滑翔机和锚雷,其模型如图 2 所示,与实物的缩比如表 1 所示。

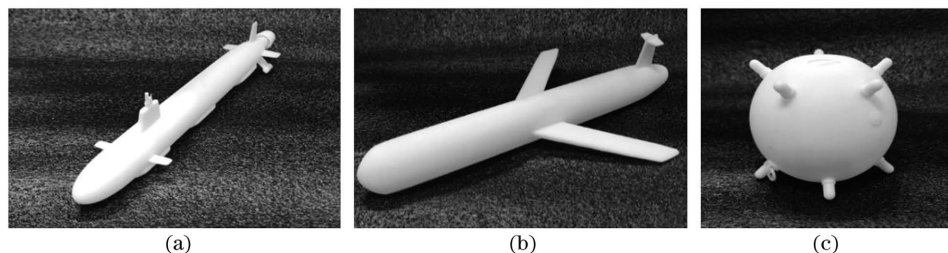


图 2 模型图。(a)潜艇模型;(b)水下滑翔机模型;(c)锚雷模型

Fig. 2 Model diagrams. (a) Submarine model; (b) underwater glider model; (c) anchor mine model

表 1 模型与实物尺寸缩比

Table 1 Size reduction ratio of models to objects

Model	Object size /m	Model size /m	Scale down
Submarine	107.6	0.300	1:358
Underwater glider	2.0	0.325	1:6
Anchor mine	0.8	0.130	1:6

2.2 真实水体环境参数模拟

海水是一种成分复杂的水溶液,温度、盐度与浊度是表征其状态的最重要参数。盐度是指海水中溶解物质质量与海水质量的比值,其与温度共同影响局部水体运动,从而影响光在水体中的传播^[7]。将每千克水中含盐 1 克定义为 1 PSU,也用 1‰表示。浊度主要由海水中未溶解、但均匀分散的悬浮物决定,在同一海域呈垂直分布,光通过时会发生吸收和散射现象^[17]。1 L 水中含有 1 mg 高岭土所构成的浊度为一个标准浊度单位,单位为 JTU。

在中国的临海中,渤海的盐度为 30 PSU,南海

的盐度与大洋水体的平均盐度一致,为 35 PSU,浊度为 1.2 JTU。本实验分别选取渤海 30 PSU 盐度、南海 35 PSU 盐度和 1.2 JTU 浊度两种真实水体环境,首先在 100 cm \times 50 cm \times 50 cm 玻璃水槽中注入 141.12 L 清水,再向其中加入 4233.6 g 盐来模拟 30 PSU 水体,搅拌均匀静置,将目标物放置在距激光雷达 80 cm 处,测得原始数据后进行滤波处理。然后,在原有的水体环境中加入 705.6 g 盐来模拟 35 PSU 水体。最后,向 35 PSU 水体中加入 0.17 g 高岭土(粒径约为 30 μ m),搅拌均匀后静置。

2.3 真实水体环境参数模拟目标激光点云数据三维重建算法

在清水水体实验中,被探测目标由重物悬挂至水槽中固定,距激光雷达 80 cm,利用激光雷达进行目标特征回波测定,收集原始点云数据。在水下目标探测过程中,水体的后向散射对三维点云数据获取的影响十分显著,其后向散射噪声主要集中在距激光雷达较近的位置,且与目标像有一个较为清晰的区分,因此采用阈值分割算法对其数据进行预处理

理,再利用折射修正和点云去噪算法进行点云重建。整体算法的流程如图 3 所示。

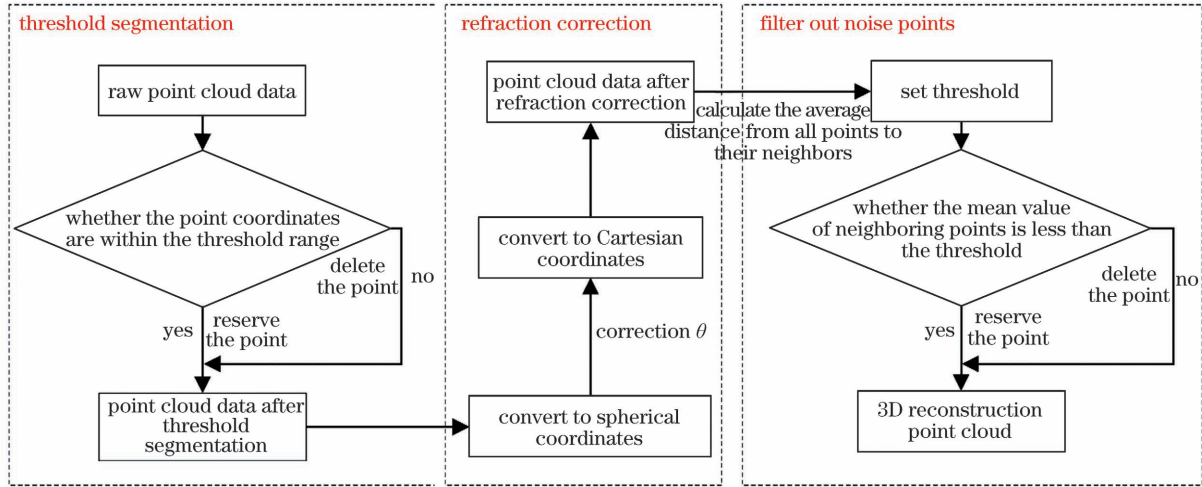


图 3 点云数据三维重建算法流程

Fig. 3 Flow chart of 3D reconstruction algorithm for point cloud data

由于激光雷达入射光线先后通过玻璃和水体这组分层介质,近红外光在超白玻璃中的折射率为 1.5229,在水体中的折射率为 1.34,因此在其界面会发生折射现象,从而影响探测精度,使探测到的点云数据球形化,因此要予以修正。激光雷达的光路如图 4 所示。

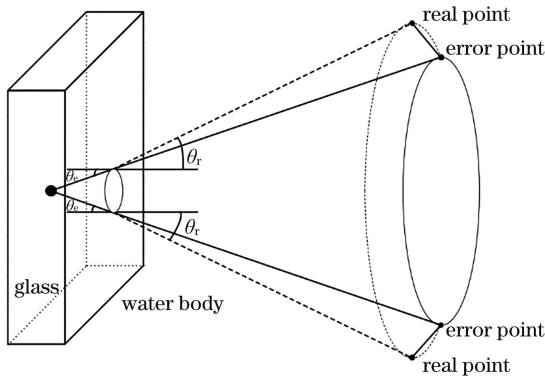


图 4 激光雷达光路

Fig. 4 Lidar optical path

点云修正的目的是将受到折射影响的原始点云数据中的误差点修正至真实坐标,将笛卡儿坐标系中的 (x_e, y_e, z_e) 点云坐标转换至 $(\varphi_e, \theta_e, r_e)$ 球坐标系中。根据折射原理,修正球坐标系中的参数 θ_e ,将修正后的球坐标点再转换到笛卡儿坐标系中显示。

已知原始坐标点为 (x_e, y_e, z_e) ,其转换至球坐标系 $(\varphi_e, \theta_e, r_e)$ 中有:

$$\begin{cases} r_e = \sqrt{x_e^2 + y_e^2 + z_e^2} \\ \theta_e = \arccos \frac{z_e}{r_e} \\ \varphi_e = \arctan \frac{y_e}{x_e} \end{cases} \quad (1)$$

在光路图的切面,设 n_g 为玻璃的折射率, n_w 为水体折射率, θ_e 为入射角, θ_r 为透射角,根据 Snell 折射定律,有

$$\theta_r = \arcsin\left(\frac{n_g \sin \theta_e}{n_w}\right) \quad (2)$$

球坐标系中的参数 r_e 由 r_g 和 r_w 两部分组成, $r_e = r_g + r_w$, r_g 为玻璃中的光程, r_w 为水体中的光程, r_g 的大小可由 $r_g = d / \cos \theta_e$ 求得,需要修正的仅为水体中的光程。因此,将球坐标系中的 $(\varphi_e, \theta_r, r_g)$ 和 $(\varphi_e, \theta_r, r_w)$ 转换至笛卡儿坐标系中,即

$$\begin{cases} x_g = r_g \sin \theta_r \cos \varphi_e \\ y_g = r_g \sin \theta_r \sin \varphi_e \\ z_g = r_g \cos \theta_r \end{cases} \quad (3)$$

$$\begin{cases} x_w = r_w \sin \theta_r \cos \varphi_e \\ y_w = r_w \sin \theta_r \sin \varphi_e \\ z_w = r_w \cos \theta_r \end{cases} \quad (4)$$

修正后的真实坐标为

$$(x_r, y_r, z_r) = (x_g, y_g, z_g) + (x_w, y_w, z_w) \quad (5)$$

经过折射修正的点云数据还要经过去噪处理。在点云去噪过程中,首先求得所有点到其相邻点的平均距离,根据所得值设置滤波阈值。当所求点的邻点均值小于所设置的阈值时,该点为有效点,否则为噪声点,将其删除。所有有效点的合集即为重建点云。

使用该算法进行点云重建时各步骤的点云数据如图 5 所示。重建后水下滑翔机的点云图像清晰地显示了水下滑翔机模型的三维形状。

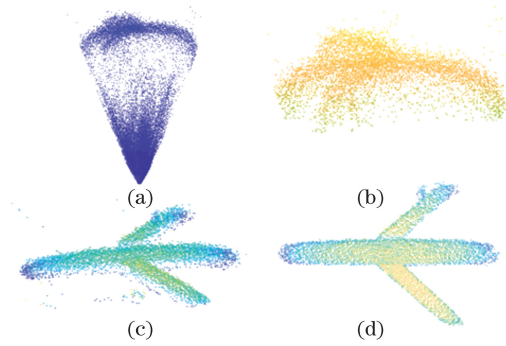


图 5 点云重建算法各步骤数据。(a)原始点云数据；(b)阈值分割后的数据；(c)折射修正后的数据；(d)点云滤波后的数据

Fig. 5 Data of each step using point cloud reconstruction algorithm. (a) Original point cloud data; (b) data after threshold segmentation; (c) data after refraction correction; (d) data after point cloud filtering

3 点云在不同真实水体中的重建

在真实水体物理特性改变对点云重建影响的研

究中,误差分析用于反映点云重建的效果。在下文的误差分析中,利用 k-d 树算法进行最近邻搜索。首先,将标准点云数据挂载到 k-d 树;然后,查询重建点云数据中的所有点与所生成 k-d 树中的最小距离;最后,将重建点云中所有点的最近点保存输出,用于误差计算。

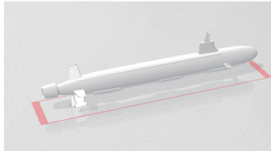
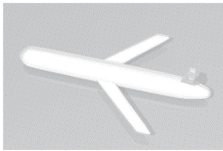

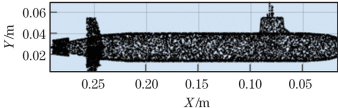
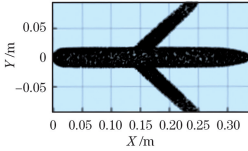
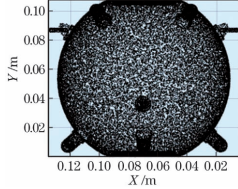
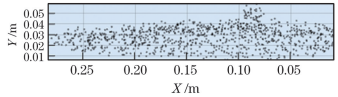
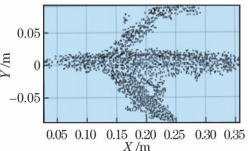
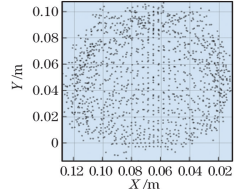
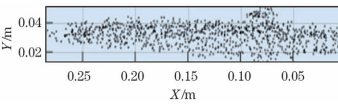
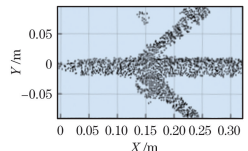
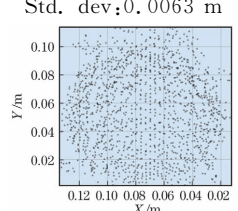
3.1 模拟水体中的盐度对点云重建的影响

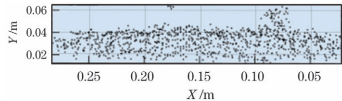
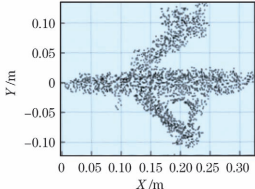
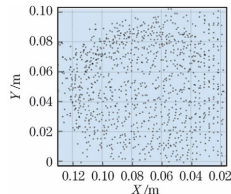
模拟渤海及南海水体中的盐度参数,重建三维点云。在本组实验中,除盐度变化外,探测距离及浊度等影响因素不变。

表 2 中每幅图像下方的数据是该点云数据与标准点云数据之间的差值误差,用于衡量点云重建效果的优劣。其中,有效点数为该组数据中所有点的总数。取其中任一点,基于 k-d 树算法求得该点在标准点云数据中的最近点,定义其两点间的距离为距离误差。距离误差中的最小值和最大值分别称作最小误差(Min. error)和最大误差(Max. error),接着计算距离误差的平均值(Avg. error)和标准差(Std. dev),将以上所有数据作为图像恢复参考。

表 2 3D 标准模型与盐度变化下的重建点云比较

Table 2 Comparison of 3D standard model and reconstructed point cloud under salinity changes

Description	Submarine	Underwater glider	Anchor mine
3D model of object			
One-sided point cloud model (standard)			
Point cloud reconstruction in clear water			
Error with standard point cloud in clear water	Number of effective points:961 Min. error:0.000192 m Max. error:0.0130 m Avg. error:0.0040 m Std. dev:0.0049 m	Number of effective points:2081 Min. error:0.000113 m Max. error:0.0452 m Avg. error:0.0064 m Std. dev:0.0083 m	Number of effective points:1320 Min. error:0.000121 m Max. error:0.0212 m Avg. error:0.0051 m Std. dev:0.0063 m
30 PSU point cloud reconstruction of Bohai Sea			

Description	Submarine	Underwater glider	Anchor mine
	Number of effective points:1037	Number of effective points:1977	Number of effective points:1454
Error with standard point cloud in the Bohai Sea	Min. error:0.000109 m	Min. error:0.000179 m	Min. error:0.000069 m
	Max. error:0.0160 m	Max. error:0.0511 m	Max. error:0.0231 m
	Avg. error:0.0044 m	Avg. error:0.0066 m	Avg. error:0.0060 m
	Std. dev:0.0052 m	Std. dev:0.0086 m	Std. dev:0.0074 m
35 PSU point cloud reconstruction of South China Sea			
	Number of effective points:1036	Number of effective points:2270	Number of effective points:1134
Error with standard point cloud in the South China Sea	Min. error:0.000186 m	Min. error:0.000195 m	Min. error:0.000097 m
	Max. error:0.0243 m	Max. error:0.0602 m	Max. error:0.0250 m
	Avg. error:0.0042 m	Avg. error:0.0096 m	Avg. error:0.0066 m
	Std. dev:0.0052 m	Std. dev:0.0131 m	Std. dev:0.0082 m

在清水水体中,三种模型最终重建的点云与标准点云的平均误差在 4~7 mm,可以视为水下被探测目标的近似点云。当水体盐度为 30 PSU 时,三种模型的平均误差总体上升不足 1 mm,其有效点数并没有明显下降,目标物的特征被复原得较好。当水体盐度为 35 PSU 时,三种模型的有效点数和平均误差既有增大也有减小。因此,盐度变化对点

云重建的总体影响略小。

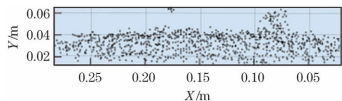
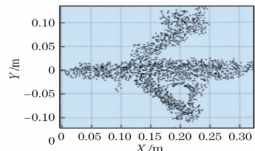
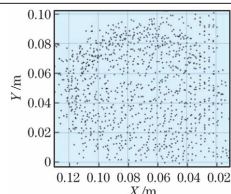
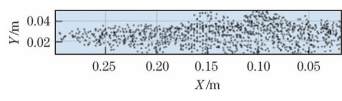
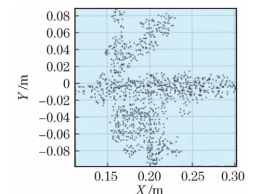
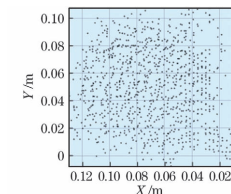
3.2 模拟南海真实水体中的浊度对点云重建的影响

在探究盐度影响的基础上,研究浊度改变对三维点云重建的影响。向 35 PSU 盐度水体中加入 0.17 g 高岭土,以模拟 1.2 JTU 浊度,再重复实验过程进行点云重建。

表 3 展示了浊度增加至 1.2 JTU 时,三种目标

表 3 3D 标准点云与浊度变化下的重建点云比较

Table 3 Comparison of 3D standard point cloud and reconstructed point cloud under turbidity changes

Description	Submarine	Underwater glider	Anchor mine
Point cloud reconstruction of South China Sea at salinity of 35 PSU			
	Number of effective points:1036	Number of effective points:2270	Number of effective points:1134
Error with standard point cloud at salinity of 35 PSU	Min. error:0.000186 m	Min. error:0.000195 m	Min. error:0.000097 m
	Max. error:0.0243 m	Max. error:0.0602 m	Max. error:0.0250 m
	Avg. error:0.0042 m	Avg. error:0.0096 m	Avg. error:0.0066 m
	Std. dev:0.0052 m	Std. dev:0.0131 m	Std. dev:0.0082 m
Point cloud reconstruction of South China Sea at salinity of 35 PSU and turbidity of 1.2 JTU			
	Number of effective points:1142	Number of effective points:1150	Number of effective points:981
Error with standard point cloud at salinity of 35 PSU and turbidity of 1.2 JTU	Min. error:0.000144 m	Min. error:0.000133 m	Min. error:0.000101 m
	Max. error:0.0226 m	Max. error:0.0391 m	Max. error:0.0337 m
	Avg. error:0.0045 m	Avg. error:0.0072 m	Avg. error:0.0089 m
	Std. dev:0.0057 m	Std. dev:0.0096 m	Std. dev:0.0111 m

物重建点云和标准点云的误差。水下滑翔机重建点云的有效点数明显下降,主要是因为浊度变大后,水体中的悬浮颗粒物变多,光束的后向散射影响变大,从而导致点云数据中的噪声点增多,被滤波算法滤除的原始点增多。其他两个模型的有效点数变化较小,但标准差均有所增大。

图 6 所示为浊度变化对点云重建的影响。由图 6 可知,随着浊度的增大,有效点数呈下降趋势,均值误差呈上升趋势。在 5 JTU 处,由于在点云滤波过程中阈值设定变大,有效点数明显减少,从而导致均值误差降低。当浊度继续增大时,即使增大滤波阈值,均值误差下降也较为有限。

综上,浊度的变化不仅影响探测精度,对有效点数的影响也不可忽视,低浊度环境下,增大滤波阈值可以降低均值误差,高浊度环境下其改善效果有限。

3.3 模拟南海真实水体中探测距离对点云重建的影响

在水下目标探测过程中,除盐度与浊度影响外,探测距离也是一个需要考虑的影响因素。在模拟南

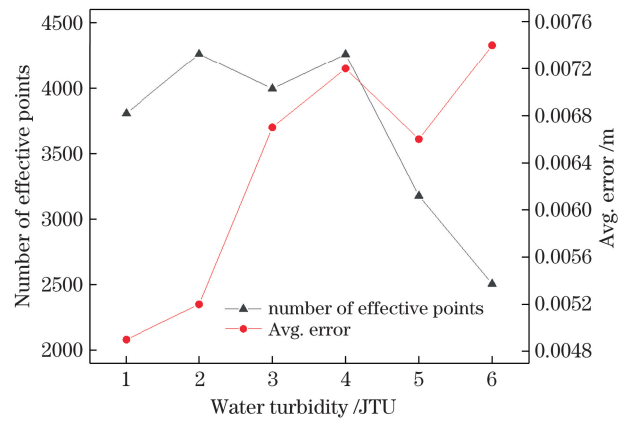


图 6 浊度变化对点云重建的影响

Fig. 6 Influence of turbidity changes on point cloud reconstruction

海 1.2 JTU 和 35 PSU 的水体中,改变目标与激光雷达的位置,距离分别取 60 cm、70 cm 和 80 cm,最终的重建效果对比如表 4 所示。

由表 4 可知,随着探测距离的增大,激光雷达的视场角不变,照射在被测目标物上的光束减小,导致有效点数减小,边缘特征变模糊,均值误差也随探测距离的增加而增大,且变化的范围超过 2 mm。

表 4 探测距离为 60 cm 和 80 cm 时南海水体中的点云重建效果对比

Table 4 Comparison of point cloud reconstruction in the South China Sea at detection distances of 60 cm and 80 cm

Description	Submarine	Underwater glider	Anchor mine
Point cloud reconstruction at 60 cm			
	Number of effective points:1933	Number of effective points:3161	Number of effective points:2219
Error with standard point cloud at 60 cm	Min. error:0.000049 m Max. error:0.0120 m Avg. error:0.0027 m Std. dev:0.0034 m	Min. error:0.0000767 m Max. error:0.0364 m Avg. error:0.0050 m Std. dev:0.0061 m	Min. error:0.000065 m Max. error:0.0203 m Avg. error:0.0042 m Std. dev:0.0053 m
Point cloud reconstruction at 80 cm			
	Number of effective points:1142	Number of effective points:1150	Number of effective points:981
Error with standard point cloud at 80 cm	Min. error:0.000044 m Max. error:0.0126 m Avg. error:0.0037 m Std. dev:0.0045 m	Min. error:0.000133 m Max. error:0.0391 m Avg. error:0.0072 m Std. dev:0.0096 m	Min. error:0.000101 m Max. error:0.0337 m Avg. error:0.0089 m Std. dev:0.0111 m

图 7 所示为探测距离变化对点云重建效果的影响。由图 7 可知,随着探测距离的增大,重建点云的有效点数呈下降趋势,重建点云与标准点云间的均

值误差呈上升趋势。有效点数减少主要是因为激光雷达的视场角固定不变,随着探测距离的增大,目标物在整个探测平面所占面积的比例下降,从而导致

接收到的反射光束数量减少,重建点云的有效点数也随之减少。均值误差上升是因为水体的后向散射产生的影响随探测距离的增大而增强,从而影响探测精度。

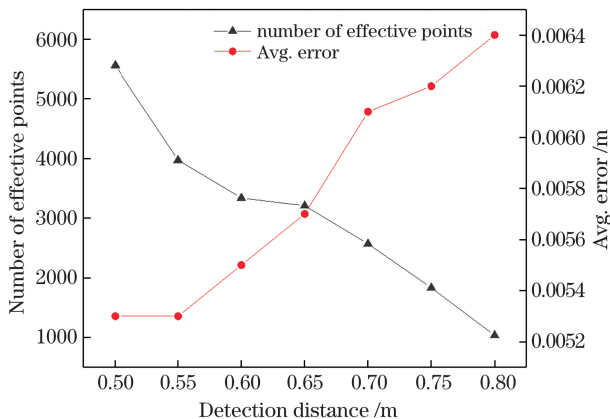


图 7 探测距离变化对点云重建的影响

Fig. 7 Influence of detection distance changes on point cloud reconstruction

4 结 论

通过量化设定盐度和浊度,模拟了渤海和南海两种真实水体环境,采用阈值分割、折射修正和点云滤波算法对所获得的原始点云数据进行重建处理,在误差分析中利用 k-d 树算法计算了重建点云与标准点云的误差,并分析其原因及影响大小。结果表明:1)盐度的改变对水下目标探测的影响较小,当盐度改变至 30 PSU 和 35 PSU,重建点云的平均误差改变范围在 1 mm 以内;2)水体浊度变化主要影响光在水下传输过程中的后向散射,导致目标点云中的噪声点数增多,从而影响成像质量;3)当目标的探测距离增大时,由于水体的衰减较大,探测效果逐渐变差,目标点云的轮廓变得模糊,有效点数呈线性减小,均值误差呈线性上升。综上,在不同水体环境的点云重建中,浊度影响占主导地位且规律性不明显,探测距离的影响可控。本研究对水下目标探测有重要的启发,可为小型水下无人滑翔机的避障和探测模块的研发提供数据参考。

参 考 文 献

- [1] Hover F S, Eustice R M, Kim A, et al. Advanced perception, navigation and planning for autonomous in-water ship hull inspection [J]. *The International Journal of Robotics Research*, 2012, 31(12): 1445-1464.
- [2] Wang M M, Wang X W, Yang Y Q, et al. Underwater de-scattering range-gated imaging based on numerical fitting and frequency domain filtering [M]//Yu H B, Liu J G, Liu L Q, et al. *Intelligent robotics and applications. Lecture notes in computer science*. Cham: Springer, 2019, 11741: 195-204.
- [3] Massot-Campos M, Oliver-Codina G. Optical sensors and methods for underwater 3D reconstruction [J]. *Sensors*, 2015, 15(12): 31525-31557.
- [4] Wang X W, Sun L, Wang M M, et al. Deblurring methods for underwater 2D and 3D range-gated imaging [J]. *Infrared and Laser Engineering*, 2020, 49(2): 0203002.
王新伟, 孙亮, 王敏敏, 等. 水下二维及三维距离选通成像去噪技术研究 [J]. *红外与激光工程*, 2020, 49(2): 0203002.
- [5] Liu X Q, Wang X W, Ren P D, et al. Automatic fishing net detection and recognition based on optical gated viewing for underwater obstacle avoidance [J]. *Optical Engineering*, 2017, 56(8): 083101.
- [6] Gan L, Zhang H. Underwater laser autonomous scanning short-range azimuth detection method based on fluid-driven [J]. *Chinese Journal of Lasers*, 2019, 46(3): 0304004.
甘霖, 张合. 基于流体驱动的水下激光自主扫描近程方位探测方法 [J]. *中国激光*, 2019, 46(3): 0304004.
- [7] He T T. Based on the Raman scattering spectra of water salinity remote sensing detection method and experimental research [D]. Xi'an: Xi'an University of Technology, 2020.
何甜甜. 基于拉曼散射光谱的水体盐度探测方法与实验研究 [D]. 西安: 西安理工大学, 2020.
- [8] Ding M J, Qiu Z F, Zhang H L, et al. Inversion algorithm for turbidity of Bohai and Yellow Seas based on NPP-VIIRS satellite data [J]. *Acta Optica Sinica*, 2019, 39(6): 0601002.
丁梦娇, 丘仲锋, 张海龙, 等. 基于 NPP-VIIRS 卫星数据的渤海黄海水体浊度反演算法研究 [J]. *光学学报*, 2019, 39(6): 0601002.
- [9] Qi R Y, Li K, Yang S H, et al. Elimination of backscatter noise of underwater LiDAR using independent component analysis algorithm [J]. *Acta Optica Sinica*, 2021, 41(4): 0401004.
齐若伊, 李坤, 杨苏辉, 等. 基于独立元分析的水下激光雷达后向散射噪声去除方法 [J]. *光学学报*, 2021, 41(4): 0401004.
- [10] Guan F, Han H W, Zhang X H. Model for visualization of laser imaging of underwater targets [J]. *Chinese Journal of Lasers*, 2020, 47(5): 0510002.
管风, 韩宏伟, 张晓晖. 水下目标激光成像的可视化模型 [J]. *中国激光*, 2020, 47(5): 0510002.

- [11] Fournier G R, Bonnier D, Forand J L, et al. Ranged-gated underwater laser imaging system [J]. *Optical Engineering*, 1993, 32(9): 2185-2190.
- [12] Busck J. Underwater 3-D optical imaging with a gated viewing laser radar [J]. *Optical Engineering*, 2005, 44(11): 116001.
- [13] Dagleish F R, Caimi F M, Britton W B, et al. Improved LLS imaging performance in scattering-dominant waters [J]. *Proceedings of SPIE*, 2009, 7317: 73170E.
- [14] Zha B T. Research on synchronous scanning underwater laser panoramic detection for short-range target [D]. Nanjing: Nanjing University of Science and Technology, 2015: 102-114.
查冰婷. 水下同步扫描周视激光近程目标探测研究 [D]. 南京: 南京理工大学, 2015: 102-114.
- [15] Xie L L, Tu D W, Zhang X, et al. Deep sea laser scanning system for underwater *in situ* measurement [C] // 2019 2nd World Conference on Mechanical Engineering and Intelligent Manufacturing (WCMEIM), November 22-24, 2019, Shanghai, China. New York: IEEE Press, 2019: 776-778.
- [16] Qian J M, Li J X, Wang Y B, et al. Underwater image recovery method based on hyperspectral polarization imaging [J]. *Optics Communications*, 2021, 484: 126691.
- [17] Ren Y Q, Wang S Z. A seawater turbidity sensor [J]. *Ocean Technology*, 2004, 23(4): 29-31.
任永琴, 王世忠. 海水浊度测量传感器研究 [J]. 海洋技术, 2004, 23(4): 29-31.

Three-Dimensional Reconstruction and Analysis of Target Laser Point Cloud Data Under Simulated Real Water Environment

Wang Mingjun^{1*}, Li Le¹, Yi Fang¹, Lei Xiaobo²

¹ School of Automation and Information Engineering, Xi'an University of Technology, Xi'an, Shaanxi 710048, China;

² Engineering Training Center, Xi'an University of Technology, Xi'an, Shaanxi 710048, China

Abstract

Objective Underwater target detection has important applications in underwater accident search and rescue, equipment maintenance, and resource exploration. Presently, underwater acoustic detection is the most common detection method, but it has limitations such as low resolution and blurred target edges, making it difficult to effectively identify the target. The underwater optical detection system perfectly compensates for the lack of underwater acoustic detection. However, physical characteristics such as salinity, temperature, and turbidity frequently affect the real ocean water environment. The underwater optical detection system's working environment is sometimes harsh, which has an impact on the system. In addition, conducting underwater detection experiments directly in the ocean is difficult. As a result, it is important to regulate changes in the physical characteristics of various water bodies in the laboratory and study their impact on detection. The findings have a substantial impact on the design and development of related equipment. In this paper, two typical sea water environments are simulated through experiments, and the effects of changes in the physical properties of salinity and turbidity and the detection distance on the three-dimensional (3D) reconstruction of the laser point cloud of underwater submarines, gliders, and anchor mines are being researched. This study can provide a reference for the development of obstacle avoidance and detection modules for small underwater unmanned gliders.

Methods We used lidar to collect the original point cloud data of targets in different water environments in the experimental glass tank. The original point cloud data obtained from the experiment was then processed using threshold segmentation, refraction correction, and point cloud denoising algorithms (Figs. 3-4), and a three-dimensional point cloud image containing only the target object was obtained (Fig. 5). In the original point cloud data, the threshold segmentation separated the target point cloud and the backscattered noise point. Refraction correction corrected the influence of refraction when crossing the medium by correcting the parameters in the spherical coordinate system. To filter out the noise points in the point cloud data, we first calculated the average distance from all points to their neighbors by point cloud denoising method and then set the filtering threshold based on the obtained value. Finally, we mounted the 3Dmax-processed standard point cloud data to the k-d tree and query the minimum distance between all points in the reconstructed point cloud data and the generated k-d tree, and save

the closest point of all points in the reconstructed point cloud. The output was used to show the error between the reconstructed point cloud and the standard point cloud.

Results and Discussions A set of point cloud reconstruction algorithms is designed in this paper (Fig. 3), and three-dimensional reconstruction point cloud images of submarines, underwater gliders, and anchor mines in various water environments are obtained. The influence of water body salinity change on the point cloud reconstruction is summarized and the data are displayed in Table 2. The results show that salinity changes have a minor impact on point cloud reconstruction. The reconstructed point cloud images of three targets exposed to turbidity changes are listed in Table 3. The mean square error and effective points between the reconstructed and standard point clouds vary with turbidity (Fig. 6). As the turbidity increases, the number of effective points shows a downward trend, and the mean error shows an upward trend. In a low turbidity environment, raising the filter threshold can help reduce mean error. The detection distance has an impact on the reconstruction of the point cloud as well. The lidar's field of view is constant. As the detection distance increases, the proportion of the target's area occupied in the entire detection plane decreases, resulting in a decrease in the number of reflected beams received, as well as a decrease in the number of effective points for reconstructing the point cloud (Fig. 7). The increase in the mean error is because the backscattering effect of the water body increases with the increase of the detection distance, which affects the detection accuracy.

Conclusions The two real water environments of the Bohai Sea and the South China Sea are simulated in this study by numerically setting the two parameters of salinity and turbidity, and experiments are conducted using this as the medium to obtain the original point cloud data, using the methods of threshold segmentation, refraction correction, and point cloud filtering for processing and reconstruction. In the follow-up error analysis, the k-d tree algorithm is used to calculate the error between the reconstructed point cloud and the standard point cloud, and the cause and impact are analyzed. The results show that: 1) the detection of underwater targets is unaffected by changes in salinity. The average error of the target changes within 1 mm in water environments of 30 PSU and 35 PSU. 2) Changes in water turbidity primarily affect light backscattering in the underwater transmission process, resulting in more noise points in the target point cloud and lowering imaging quality. 3) When the target's detection distance is fixedly increased, the detection effect gradually deteriorates due to the large attenuation of the water body, and the target point contour of the cloud becomes blurred. The mean error effect increases as the number of effective point clouds decreases. In conclusion, the turbidity influence is dominant in point cloud reconstruction under different water environments, the regularity is not obvious, and the detection distance influence is controllable.

Key words image processing; laser point cloud; underwater detection; real water simulation; three-dimensional point cloud reconstruction; error analysis